© 2016. Published by The Company of Biologists Ltd | Journal of Experimental Biology (2016) 219, 3810-3821 doi:10.1242/jeb.143537

RESEARCH ARTICLE

The long road to steady state in gas exchange: metabolic and ventilatory responses to hypercapnia and hypoxia in Cuvier's dwarf caiman

Christian Lind Malte*, Hans Malte and Tobias Wang

ABSTRACT

Animals with intermittent lung ventilation and those exposed to hypoxia and hypercapnia will experience fluctuations in the bodily O_2 and CO_2 stores, but the magnitude and duration of these changes are not well understood amongst ectotherms. Using the changes in the respiratory exchange ratio (RER; CO_2 excretion divided by O_2 uptake) as a proxy for changes in bodily gas stores, we quantified time constants in response to hypoxia and hypercapnia in Cuvier's dwarf caiman. We confirm distinct and prolonged changes in RER during and after exposure to hypoxia or hypercapnia. Gas exchange transients were evaluated in reference to predictions from a two-compartment model of CO_2 exchange to quantify the effects of the levels of hypoxia and hypercapnia, duration of hypercapnia (30–300 min) and body temperature (23 versus 33°C). For hypercapnia, the transients could be adequately fitted by two-phase exponential functions, and slow time constants (after 300 min hypercapnia) concurred reasonably well with modelling predictions. The slow time constants for the decays after hypercapnia were not affected by the level of hypercapnia, but they increased (especially at 23°C) with exposure time, possibly indicating a temporal and slow recruitment of tissues for CO_2 storage. In contrast to modelling predictions, elevated body temperature did not reduce the time constants, probably reflecting similar ventilation rates in transients at 23 and 33°C. Our study reveals that attainment of steady state for gas exchange requires considerable time and this has important implications for designing experimental protocols when studying ventilatory control and conducting respirometry.

KEY WORDS: Steady state, Time constants, Gas exchange, Hypoxia, Hypercapnia, Reptile

INTRODUCTION

Fluctuations in bodily O_2 and CO_2 stores are particularly pronounced in animals with intermittent ventilation patterns, such as reptiles and diving mammals, and bodily gas stores obviously also change when animals are exposed to hypoxia or hypercapnia (Burggren and Shelton, 1979; Glass and Johansen, 1979; Glass and Wood, 1983; Milsom, 1991; Shelton and Boutilier, 1982). The magnitude and temporal development of these changes depend critically on the ventilatory and circulatory responses (Malte et al., 2016b), but, although ventilatory responses to hypercapnia and hypoxia have been described in many reptiles (for reviews see Milsom, 1991; Shelton et al., 2010; Wang et al., 1998), the associated transients in bodily gas stores have not been quantified. Consequently, it is not clear how long it takes to achieve a steady state for gas exchange, i.e. the time required to readjust bodily gas stores during and after hypoxia or hypercapnia. Knowledge of the time constants quantifying the transients between steady states is pivotal in the design of experimental protocols for estimating tissue gas exchange as well as in the interpretation of the ventilatory responses, particularly in cases of repeated exposures to intermittent periods of hypoxia and/or hypercapnia (e.g. Porteus et al., 2011). The time constants also provide useful insight into the resistances/conductances to gas transport as well as the bodily storage capacity for O_2 and CO_2 (Cherniack and Longobardo, 1970; Farhi and Rahn, 1955; Farhi and Rahn, 1960).

In the simplest possible model, the time constant is given by the product of resistance and total capacitance/storage capacity corresponding to an exponential wash-in and wash-out of a single well-stirred compartment (Farhi and Rahn, 1955, 1960). However, tissues, blood and lungs constitute separate distinct compartments linked by limiting transport processes (perfusion and diffusion). Thus, a two-compartment model with a merged venous–tissue compartment and an arterial–pulmonary compartment (see Appendix) offers a better, albeit still simplistic, approach (Farhi and Rahn, 1960; Longobardo et al., 1967) (see also Shelton and Croghan, 1988 for a slightly different numerical model for bimodal breathers). Here, gas transport from the tissues to the environment is dictated by two resistances arranged in series associated with blood and air convection, and the solution involves a two-phase exponential function with a fast and a slow time constant (τ_1 and τ_2, respectively), determined by these resistances and capacities of the compartments (see Appendix). Given the high bodily storage capacity for CO_2 compared to O_2, readjustments of CO_2 stores have longer time constants than O_2, and CO_2 transport therefore dominates the overall time constant for the transients between steady states (Farhi and Rahn, 1955); this is also well documented in periodic ventilation (Boutilier, 1990; Boutilier et al., 2001; Garland and Milsom, 1994).

The two-compartment model predicts that time constants decrease when blood flow and ventilation rates increase and vice versa (see Appendix and Fig. S1). Hence, time constants for ectotherms are expectedly longer than for endotherms given the lower rates of ventilation and blood flow along with the potential for intra-cardiac shunts. However, the model would predict that time constants are reduced at elevated body temperature as rates of blood flow and ventilation increase (Dejours, 1981; Jackson, 1971; Smith, 1975), whereas the capacitance coefficients are moderately reduced (Dejours, 1981; Weinstein et al., 1986).

Zoophysiology, Department of Bioscience, Aarhus University, Aarhus C 8000, Denmark.

*Author for correspondence (christian.malte@bios.au.dk)

C.L.M., 0000-0002-7003-6370

Received 22 May 2016; Accepted 31 August 2016

Journal of Experimental Biology

Journal of Experimental Biology (2016) 219, 3810-3821 doi:10.1242/jeb.143537

List of symbols and abbreviations

C_a	arterial–lung storage capacity
C_v	venous–tissue storage capacity
f_R	respiratory frequency
Pa_{CO_2}	arterial P_{CO_2}
P_{CO_2}	partial pressure of CO_2
$P_{I CO_2}$	inspired P_{CO_2}
P_{O_2}	partial pressure of O_2
Pv_{CO_2}	venous P_{CO_2}
$\dot{Q}$	blood flow rate
RER	respiratory exchange ratio
R_{perf}	perfusive resistance
R_{vent}	ventilatory resistance
V_a	volume of arterial blood
V_A	volume of lung
$\dot{V}_A$	alveolar/effective ventilation rate
$\dot{V}_{CO_2}$	tissue CO_2 production rate
$\dot{V}_{CO_2,b}$	lung CO_2 excretion rate
$\dot{V}_E$	ventilation rate
$\dot{V}_{O_2}$	tissue O_2 consumption rate
$\dot{V}_{O_2,b}$	lung O_2 uptake rate
V_T	tidal volume
V_{Tis}	size of tissues
V_v	volume of venous blood
β_b	blood capacitance coefficient
β_g	air capacitance coefficient
β_T	tissue capacitance coefficient
τ	time constant
τ_1	fast time constant
τ_2	slow time constant

Here, we determine time constants for changes in gas exchange (and thus, indirectly, bodily gas stores) and ventilatory responses to hypoxia and hypercapnia in Cuvier's dwarf caimans (*Paleosuchus palpebrosus*), a suitable species for simultaneous measurements of gas exchange and ventilation using pneumotachography (Glass et al., 1978; Wang and Warburton, 1995). Given the present difficulty in acquiring precise blood gas values at a high sampling rate (Malte et al., 2014), we used changes in RER (CO_2 excretion divided by O_2 uptake) as a proxy for changes in bodily gas stores because RER ideally will approach a steady state equal to the respiratory quotient [RQ; tissue CO_2 production divided by O_2 consumption (Farhi and Rahn, 1955)]. The experimentally acquired time constants were evaluated with reference to predictions from a two-compartment model of CO_2 exchange testing the effect of intensity of hypercapnia (inspired P_{CO_2}) and hypoxia (inspired P_{O_2}), duration of hypercapnia (30–300 min), and the effect of temperature (23 versus 33°C). We hypothesize that the slow time constants decrease at higher body temperature in accordance with modelling predictions, but increase following a longer duration of hypercapnia, possibly due to a temporal increase in tissue apparent/effective storage capacity.

MATERIALS AND METHODS

Animals and instrumentation

Experiments were performed on six juvenile Cuvier's dwarf caiman (*Paleosuchus palpebrosus*, Cuvier 1807) of unknown sex with a mean body mass (±s.e.m.) of 0.93±0.05 kg housed at 25–27°C in an aquarium with a platform allowing basking under a heating lamp. During measurements they were placed in a dark box in a heating cabinet at 23 or 33°C to minimize disturbance. Animals were fitted with a face-mask glued to the head with fast hardening epoxy glue as previously described by Glass et al. (1978) and Wang and Warburton (1995). Animals were placed at test temperature at least 16–20 h before measurements in order for the bodily CO_2 stores to adjust to the new body temperature (e.g. Stinner et al., 1998; Stinner and Wardle, 1988). The number of animals was chosen as to obtain sufficient power for statistical analyses. Experiments were conducted in compliance with the rules of the Danish Animal Experiments Inspectorate.

Measurements of gas exchange and ventilation

The experimental setup (Fig. 1A) for measurements of gas exchange and ventilation was similar to previous descriptions (Wang and Warburton, 1995). One end of the T-piece of the face-mask was connected to a side-tube connected to a mass flow meter (Sierra Instruments, Inc.), whilst the other was connected to CO_2 and O_2 analysers (AEI Technologies) and a steady flow was pulled through the side tube using two parallel arranged flow controllers (R2 Flow Control from AEI Technologies and the other custom-made). The flow of 500–900 ml standard temperature and pressure (STP) min^{-1} was sufficient to minimize rebreathing of exhaled gases. Ventilation was measured directly as the change in flow through the mass flow meter of the side tube upstream of the animal following expiration (negative deflection) and inspiration (positive deflection), which was verified by injections of known volumes into the circuit. CO_2 and O_2 analysers were calibrated using 100% N_2, 21% O_2 (balance 79% N_2) and 5% CO_2 (balance 74% N_2 and 21% O_2) prepared with Wösthoff gas mixing pumps (Bochum, Germany) in parallel that could deliver a flow surpassing the suction flow through the circuit. Given the constant flow pulled downstream from the mask and into the O_2 and CO_2 sensors, gas exchange per breath could be calculated as the product of the integrated gas fraction below or above baseline and the flow rate. This was verified as previously described (Wang and Warburton, 1995) by simulating exhalations with known gas compositions via injecting known volumes of O_2 and CO_2 into the circuit with the mask glued to a cast, thereby establishing tight (R^2=0.999) proportional relations between the calculated volumes and the injected volumes (slope of 0.96). All data was collected using BioPac data acquisition systems.

Protocols

We carried out several protocols on separate days to measure gas exchange and ventilation in response to hypercapnia and hypoxia. In all protocols, animals were instrumented with the face mask on the previous day before measurements. After calibrating the O_2 and CO_2 analysers, the animal was connected to the circuit with the suction flow and allowed to rest for at least 2 h in order to acquire control values of ventilation and gas exchange.

Response to different inspired P_{CO_2} and P_{O_2} at 23°C

In a randomized fashion, on one day, the animal was exposed to hypoxia (either 5% or 10% O_2, balance N_2) for 1 h followed by at least 2 h re-exposure to room air. Similarly, on the other day, the animal was exposed to hypercapnia (either 1%, 2% or 4% CO_2 balanced with N_2 and O_2 to produce the percentage of O_2 in room air) for 1.5 h followed by at least 1.5 h exposure to room air.

Response to different durations of hypercapnia at different temperatures (23°C and 33°C)

Two different experimental protocols were conducted on separate days in a randomized fashion measuring the response to varying

Journal of Experimental Biology (2016) 219, 3810-3821 doi:10.1242/jeb.143537

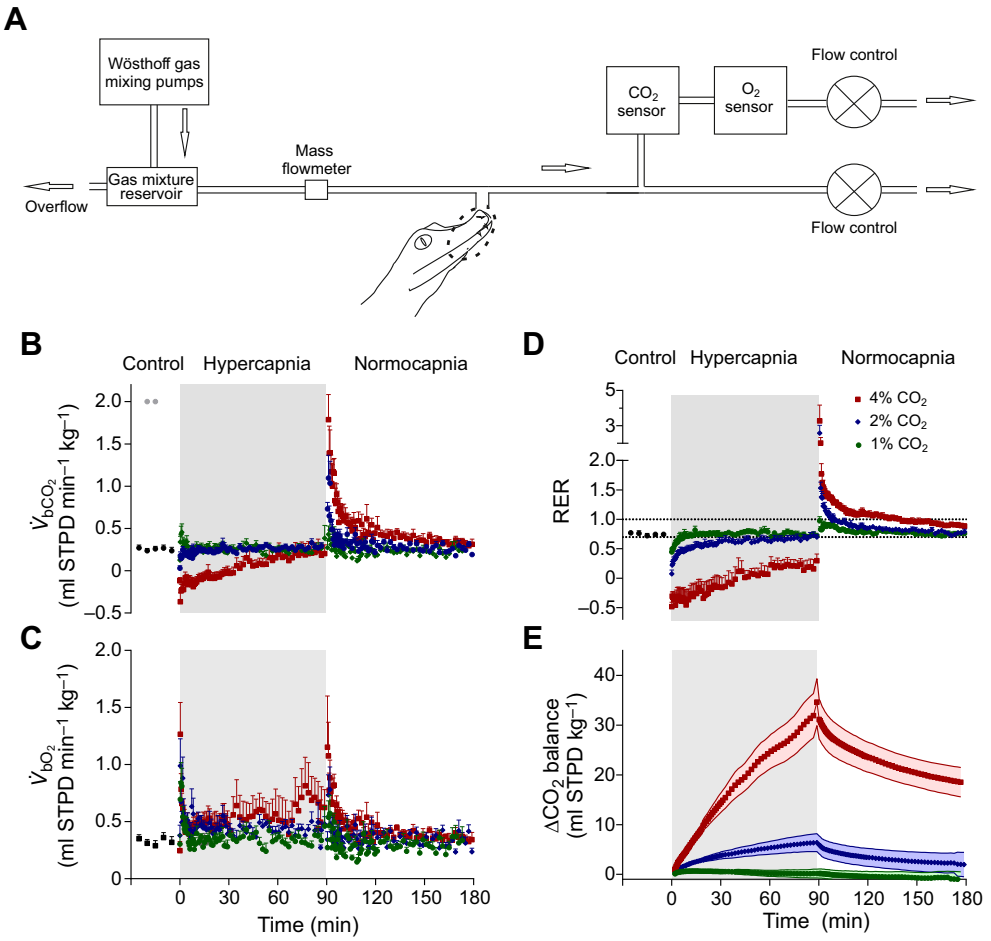

Fig. 1. Experimental setup and gas exchange responses to hypercapnia. Gas exchange upon and following hypercapnia. (A) Schematic representation of the experimental setup. (B–D) $\dot{V}_{CO_2,b}$, $\dot{V}_{O_2,b}$ and respiratory exchange ratio (RER) (means+s.e.m.), respectively, before, during and after exposure to hypercapnia at the indicated levels. The dotted lines in D indicate the physiological RQ range (0.7–1). (E) The estimated changes in CO_2 balance (means±s.e.m.) during and after hypercapnia. See Table 2 for fitted parameters made to combined data from all animals with weighted least-squares method and Fig. 2A for fitted slow time constants with robust method and Monte Carlo-acquired confidence intervals. *N*=6.

durations of hypercapnia at 23°C and 33°C. On one day, the animal was exposed to 3% CO_2 [with approximately 20.6% O_2 (room air with ambient humidity), balance N_2] for either 30 min or 90 min in a randomized fashion, followed by re-exposure to room air for either 90 min or 180, respectively. On the other day, the animal was exposed to 3% CO_2 [with 20.6% O_2 (room air with ambient humidity), balance N_2] for 300 min followed by ideally 300 min exposure to room air.

Data analysis

All analyses of breath-to-breath gas exchange and ventilation was carried out in Mathematica 7.0 (Wolfram Research, Inc.). O_2 and CO_2 exchange per breath was calculated as the product of the integrated gas fraction below or above baseline, respectively, and the rate of air flow downstream of the mask. Likewise, tidal volume was calculated as the integrated flow signal from the mass flow meter during expiration and inspiration. Given the high flow rate, the long experimental protocols and the need for fast response times of the O_2 and CO_2 signals, we did not dry the expired air before it entered the O_2 and CO_2 sensor. However, the expired gas was assumed to be saturated with water vapor and we either saturated the inspired air with water vapor or measured room air humidity (50–60% during the days of experimentation) so that we could express gas exchange as standard temperature and pressure, dry (STPD). Not drying the expired gas could maximally (and unrealistically) lead to an overestimation of STPD gas exchange of around 1% depending on the barometric pressure. The intermittent ventilation patterns of crocodiles (and other reptiles) complicate representation of the combined time-based data for gas exchange and ventilation as means with s.e.m. However, this was circumvented by calculating mean values for appropriate time intervals for the individually based event data by using linear interpolation. The time intervals were chosen in order to minimize interfering with the dynamics of the individually based data.

In cases where the peaks in the expired O_2 and CO_2 traces were not sufficiently distinguishable from a baseline level, making integration too uncertain, the animal was excluded from the specific analysis.

Nonlinear regressions

To RER data upon and following hypercapnia, we fitted one- or two-phase exponential functions to the combined-event-based data using both weighted least squares (each y value weighted by $1/y^2$) and robust nonlinear regression (Motulsky and Christopoulos, 2004; Motulsky and Brown, 2006). If the two-phase exponential fit was ambiguous, we tried fitting a one-phase exponential instead. Confidence intervals for the slow time constants for the robust fits were acquired by means of Monte Carlo simulations using the standard deviation of the residuals for the robust fit (RSDR) and letting the residuals follow a Lorentzian distribution. To the simulated data, robust nonlinear regressions were conducted where the plateau was constrained to lie above 0.7 (i.e. the lower limit of RQ). We carried out 1000 simulations for each confidence interval. Finally, we also fitted event-based robust nonlinear regressions to data from individual animals which could be compared using either a one- or two-way ANOVA testing the

Journal of Experimental Biology (2016) 219, 3810-3821 doi:10.1242/jeb.143537

effect of inspired percentage CO_2, and the duration of hypercapnia and body temperature, respectively.

Response to different levels of hypoxia and hypercapnia at 23°C

The effects of hypercapnia on ventilatory parameters were evaluated with a repeated measures ANOVA (α=0.05), where mean values for the initial control period were compared to overall mean values for the last 20 min of hypercapnia. Similarly, repeated measures ANOVA were used to compare mean $\dot{V}_E$ and V_T for the decay after exposure to 2, 3 and 4% CO_2.

Paired *t*-tests were used to compare ventilatory parameters and gas exchange for control and during hypoxia. Here, values before hypoxia were compared to mean values for the last 20 min (for ventilation data) or 10 min (for gas exchange data) during hypoxia. Following return to normoxia after hypoxia, we did not make exponential fits given that data did not appear to fit a simple one- or two-phase exponential function. Instead, we evaluated the time required to reach ∼63% of the pre-hypoxic control RER value for each animal by simply fitting a polynomial function for the relevant time domain. The time constants for 5% and 10% O_2 exposures were compared using a Wilcoxon matched-pairs signed-rank test.

Response to different durations of hypercapnia at different temperatures (23°C and 33°C)

The effects of temperature and hypercapnia on ventilatory responses during the last 20 min of hypercapnia (for the 300 min exposure) were compared to control using a two-way ANOVA (without repeated measures due to missing data points). Similarly, a two-way ANOVA was performed to test for differences between overall mean $\dot{V}_E$ and V_T for the first 90 min of the decays after exposure to the different durations of hypercapnia (30, 90 and 300 min) at 23 and 33°C. In general, data was log-transformed if necessary. All statistical analyses were performed in GraphPad Prism (GraphPad Software).

Estimates of changes in O_2 and CO_2 balance of the body

Crude estimates of the changes in bodily O_2 and CO_2 stores were obtained from the gas exchange data. The change in CO_2 content of the body from any time t_0 to t_0+t [$\Delta V_{CO_2,tot}(t_0+t)$] is given by the integrated difference between CO_2 production ($\dot{V}_{CO_2}$) and excretion ($\dot{V}_{CO_2,b}$) rate:

$$\Delta V_{CO_2,tot}(t_0+t) = \int_{t_0}^{t+t_0} [\dot{V}_{CO_2}(t) - \dot{V}_{CO_2,b}(t)]\mathrm{d}t. \quad (1)$$

Upon and following hypercapnia exposure, it is assumed that O_2 uptake ($\dot{V}_{O_2,b}$) always equals O_2 consumption ($\dot{V}_{O_2}$) (which will at best be a rough approximation), so that CO_2 production can be calculated as the product of steady state RER (i.e. RQ) and O_2 uptake ($\dot{V}_{O_2,b}$):

$$\Delta V_{CO_2,tot}(t_0+t) = \int_{t_0}^{t+t_0} [\mathrm{RQ}\dot{V}_{O_2,b}(t) - \dot{V}_{CO_2,b}(t)]\mathrm{d}t. \quad (2)$$

The assumption that O_2 uptake always represents O_2 consumption does not hold during hypoxia exposure, in which transient changes in bodily O_2 stores are inevitable. Here, changes in CO_2 balance were estimated according to Eqn 1, where CO_2 production was assumed to equal steady state CO_2 excretion. The change in O_2 content of the body from any time t_0 to t+t_0 [$\Delta V_{O_2,tot}(t_0+t)$] is given by the integrated difference between O_2 uptake and consumption:

$$\Delta V_{O_2,tot}(t_0+t) = \int_{t_0}^{t+t_0} [\dot{V}_{O_2,b}(t) - \dot{V}_{O_2}(t)]\mathrm{d}t. \quad (3)$$

Upon and following hypoxia exposure it was assumed that O_2 consumption is constant and equal to the pre-hypoxic control values. However, this assumption would clearly be invalid in the case of hypoxic hypometabolism/depression (e.g. Hicks and Wang, 1999).

Two-compartment model of the bodily CO_2 stores

Under the assumption of absence of diffusion limitation, shunts and spatial in-homogeneities and using joined, well stirred venous blood-tissue as well as lung-arterial compartments (similar to Longobardo et al., 1967; see also Farhi and Rahn, 1955, 1960), we derived a model for the CO_2 stores of the body (see Appendix for differential equations). For constancy of parameters (storage capacities, resistances and metabolic rate), the model has an analytic solution, where dynamics of pulmonary CO_2 exchange {abbreviated $\dot{V}_{CO_2,b}$ to distinguish it from steady state [i.e. CO_2 production ($\dot{V}_{CO_2}$)]} can be quantified by a two-phase exponential function:

$$\dot{V}_{CO_2,b}(t) = \dot{V}_{CO_2} + A_1\exp\left(-\frac{t}{\tau_1}\right) + A_2\exp\left(-\frac{t}{\tau_2}\right). \quad (4)$$

Here, A_1 and A_2 are the span of the disturbance from steady state associated with the fast time constant (τ_1) and the slow time constant (τ_2), respectively. See Table 1 for expressions for the spans and time constants determined by the resistances to gas transport (denoted *R*) and the storage capacities of the compartments (denoted *C*).

RESULTS

Model predictions

Fig. S1A,B shows density plots for the fast and slow time constant divided by the product of total storage capacity (C_{tot}=C_a+C_v) and resistance (R_{tot}=R_{perf}+R_{vent}) (see Table 1 for abbreviations etc.). Here, the *x*-axis is the fraction of the total resistance attributed to ventilation (R_{vent}/R_{tot}) and *y*-axis is the fraction of the total storage capacity attributed to the arterial–lung compartment (C_a/C_{tot}). It is evident that, as long as the total storage capacity is distributed at two distinct compartments, and if there is a finite convective resistance for transport between the compartments, the dynamics of the CO_2 stores will be characterized by two distinct time constants. Furthermore, for a given total resistance, the slow time constants becomes longer if the ventilatory resistance dominates in combination with high relative venous–tissue storage capacity and vice versa.

Increasing both the total storage capacity, for a given distribution between the compartments, and the total resistance, the fast and the slow time constant will increase. Fig. S1C,D illustrate how the fast and slow time constants are affected by the ventilatory and perfusive resistance (R_{vent} and R_{perf}) via changes in alveolar ventilation (*x*-axis) and blood flow (*y*-axis) (see legend for values of input parameters). Hence, increasing both blood flow and ventilation reduce the time constants in a hyperbolic-like manner and, conversely, if blood flow and/or ventilation approach zero the slow time constant approaches infinity. It is also seen that, for typical normal blood flow rates of an ectotherm, increasing ventilation mostly affects the slow time constant because the overall transport is mostly limited by ventilation. For a broad range of blood flow values (20–50 ml min^{-1} kg^{-1}) and

Journal of Experimental Biology (2016) 219, 3810-3821 doi:10.1242/jeb.143537

Table 1. Model parameters quantified by the input parameters and initial conditions

Model parameter	Equation
Total span in $\dot{V}_{CO_2,b}$ attributed to fast phase (A_1)	$A_1 = \frac{\tau_1\{\tau_2[-Pa_{CO_2,i}(R_{vent}+R_{perf}) + P_{ICO_2}R_{perf} + Pv_{CO_2,i}R_{vent}] - C_aR_{perf}R_{vent}(-Pa_{CO_2,i} + P_{ICO_2} + R_{vent}\dot{V}_{CO_2})\}}{C_aR_{perf}R_{vent}^2(\tau_1-\tau_2)}$
Total span in $\dot{V}_{CO_2,b}$ attributed to slow phase (A_2)	$A_2 = \frac{\tau_2\{C_aR_{perf}R_{vent}(-Pa_{CO_2,i} + P_{ICO_2} + R_{vent}\dot{V}_{CO_2}) + \tau_1[Pa_{CO_2,i}(R_{vent}+R_{perf}) - P_{ICO_2}R_{perf} - Pv_{CO_2,i}R_{vent}]\}}{C_aR_{perf}R_{vent}^2(\tau_1-\tau_2)}$
The fast and slow time constant (τ_1 and τ_2)	$\tau_1 = -\frac{2}{-b-c-d-\sqrt{-4bd+(b+c+d)^2}}$, $\tau_2 = -\frac{2}{-b-c-d+\sqrt{-4bd+(b+c+d)^2}}$
Lumped parameters	$a = \frac{\dot{V}_{CO_2}}{C_v}$, $b = \frac{1}{R_{perf}C_v}$, $c = \frac{1}{R_{perf}C_a}$, $d = \frac{1}{R_{vent}C_a}$
Ventilatory resistance and blood convective/perfusive resistance (R_{vent} and R_{perf}, respectively) and total resistance (R_{tot})	$R_{vent} = \frac{1}{\dot{V}_A\beta_g}$, $R_{perf} = \frac{1}{\dot{Q}\beta_b}$, $R_{tot} = R_{perf} + R_{vent}$
Storage capacity of lung–arterial compartment (C_a) and venous–tissue compartment (C_v) and total storage capacity (C_{tot})	$C_a = V_a\beta_b + V_A\beta_g$, $C_v = V_v\beta_b + V_{Tis}\beta_T$, $C_{tot} = C_a + C_v$

V refers to size of compartment, β is the capacitance coefficient (where b refers to blood and g refers to air) and the subscripts a, A, v and Tis refer to arterial, lung, venous and tissues, respectively. P_{ICO_2} is inspired partial pressure of CO_2, $\dot{Q}$ is cardiac output, and subscript i refers to initial conditions.

'alveolar' ventilation (10–30 ml min^{-1} kg^{-1}) in a reptile, the model predicts fast and slow time constants in the range ~0.5–1.5 min and ~20–120 min, respectively (assuming a range of the available tissues' storage capacities, giving total storage capacity ~0.77–1.5 ml STPD mmHg^{-1} kg^{-1} animal; see legend of Fig. S1).

The model predicts that time constants are determined only by the resistances and storage capacities (see Table 1), and hence time constants would ideally be predicted to be independent of the intensity (inspired P_{CO_2}) and duration of hypercapnia for the same rates of ventilation (and blood flow) when storage capacities are constant. Furthermore, the model predicts that time constants are reduced at elevated body temperature given the effects of body temperature on rates of ventilation and blood flow (Dejours, 1981; Jackson, 1971; Smith, 1975).

Effects of inspired P_{CO_2}

Fig. 1 shows rates of CO_2 excretion ($\dot{V}_{CO_2,b}$, Fig. 1B), O_2 uptake ($\dot{V}_{O_2,b}$, Fig. 1C) and RER (Fig. 1D), as well as the estimated change in CO_2 balance (Fig. 1E) before, during and after exposure to three different levels of hypercapnia. RER was reduced immediately upon exposure to hypercapnia, and RER could be quantified by a one- or two-phase exponential function for 1 and 2% CO_2 (see 'on' in Table 2A,B); however, no reliable fit could be made to data at 4% CO_2.The transient reduction in RER was due to reduced $\dot{V}_{CO_2,b}$ in combination with a tendency for elevated $\dot{V}_{O_2,b}$. Upon exposure to 4% CO_2, $\dot{V}_{CO_2,b}$ was negative for around 30 min, where all inspired and metabolically produced CO_2 accumulated in the body instead of being eliminated, leading to large retention and accumulation of CO_2 (Fig. 1E). Upon re-exposure to normocapnia, RER was transiently elevated due to elevated $\dot{V}_{CO_2,b}$ and the time course for RER could be quantified by two-phase exponential decays for 2, 3 and 4% CO_2 and one-phase exponential decay for 1% CO_2 (see 'off' in Table 2A–C) (notice that the decay for 3% CO_2 was a part of another protocol and is shown in Fig. 7). There was no effect of inspired percentage CO_2 on the slow time constant for the decays, neither when comparing individual fits (P=0.314, one-way repeated measures ANOVA; not shown) or when simply comparing overlap between the confidence intervals acquired for the combined fits for all animals using (weighted) least squares or robust fits (with Monte Carlo confidence intervals) (Fig. 2A, where only the results for robust fits are shown). Neither mean $\dot{V}_E$ or V_T were significantly different for the decays (P=0.732 and P=0.273, respectively, one-way repeated measures ANOVA) after 2, 3 and 4% CO_2. The ventilatory response to hypercapnia is shown in Fig. 3: whereas hypercapnia significantly affected tidal volume (V_T) (P=0.002, one-way repeated measures ANOVA), there was no significant effect of hypercapnia on breathing frequency (f_R) or minute ventilation ($\dot{V}_E$) (P=0.381 and P=0.156, respectively, one-way repeated measures ANOVA) even though there was a clear tendency for elevated $\dot{V}_E$ at 2 and 4% CO_2. However, the variability of the ventilatory response to 4% CO_2 was very high and in some animals $\dot{V}_E$ was vastly elevated, whereas, in others, f_R was lowered, leading to constant or even slightly reduced $\dot{V}_E$.

Effects of inspired P_{O_2}

Fig. 4 shows the results for gas exchange and the estimated changes in O_2 and CO_2 balance during control, exposure to hypoxia (5 and 10% O_2) and following re-exposure to normoxia. During the initial phase of hypoxia, O_2 was transiently eliminated, leading to reduced O_2 stores of the body (Fig. 4B,C), and therefore RER values were initially negative and then increased above control values (Fig. 4A). Both $\dot{V}_{O_2,b}$ and RER approached a plateau and at the end of 10% O_2 exposure: $\dot{V}_{O_2,b}$, $\dot{V}_{CO_2,b}$ and RER were not significantly different from control (P=0.079, P=0.363, P=0.140, t-tests). However, RER remained significantly elevated at 5% O_2 compared to control (P=0.002, t-test) due to significantly elevated $\dot{V}_{CO_2,b}$ (P=0.0003, t-test), whereas $\dot{V}_{O_2,b}$ was only slightly, but significantly, higher than pre-hypoxic values (P=0.029, t-test). Therefore, the estimated change in CO_2 balance at 5% O_2 was negative (i.e. the CO_2 store of the body was reduced; Fig. 4F). Upon re-exposure to normoxia, RER values dropped to near zero because of elevated $\dot{V}_{O_2,b}$ (see Fig. 4A and D, which is a zoomed-in version of the re-exposure to normoxia), leading to estimated restoration of bodily O_2 stores (Fig. 5C). Furthermore, upon returning to normoxia from 5% O_2, $\dot{V}_{CO_2,b}$ tended to decline, leading to estimated CO_2 retention (Fig. 4F). $\dot{V}_{O_2,b}$, $\dot{V}_{CO_2,b}$ and RER gradually approached a steady state in a non-linear fashion upon re-exposure to normoxia and the estimated time to reach ~63% of pre-hypoxic control RER after 5% CO_2 (40.4±10.2 min) was significantly longer than after 10% O_2 (9.0±2.0 min) (P=0.031, Wilcoxon matched pairs).

Journal of Experimental Biology (2016) 219, 3810-3821 doi:10.1242/jeb.143537

Table 2. Fitted parameter estimates

(A) Varying inspired P_{CO_2}

Treatment and model	Initial RER value	Final RER value	τ (min)
1% CO_2: on, one-phase association	0.338 (0.3069 to 0.3695)	0.717 (0.703 to 0.731)	7.43 (6.079 to 9.554)
1% CO_2: off, one-phase decay	0.944 (0.9016 to 0.9866)	0.765 (0.7513 to 0.7784)	12.29 (8.451 to 22.49)

(B) Varying inspired P_{CO_2}

Treatment and model	Initial RER value	Final RER value	Fraction of RER span for τ_1	τ_1 (min)	τ_2 (min)
2% CO_2: on, two-phase association	0.0179 (−0.071 to 0.1070)	0.664 (0.643 to 0.685)	0.5429 (0.4373 to 0.6485)	1.211 (0.741 to 3.300)	20.491 (14.684 to 33.898)
2% CO_2: off, two-phase decay	3.401 (3.081 to 3.720)	0.779 (0.7636 to 0.7937)	0.8273 (0.8032 to 0.8513)	0.4918 (0.4256 to 0.5822)	19.54 (16.68 to 23.59)
4% CO_2: off, two-phase decay	2.634 (2.391 to 2.877)	0.869 (0.8521 to 0.8864)	0.6827 (0.6324 to 0.7330)	0.7587 (0.5811 to 1.093)	19.77 (16.85 to 23.91)

(C) Varying duration of hypercapnia and body temperature

Treatment and model	Initial RER value	Final RER value	Fraction of RER span for τ_1	τ_1 (min)	τ_2 (min)
23°C, 300 min of 3% CO_2: off, two-phase decay	4.910 (4.499 to 5.321)	0.8362 (0.8278 to 0.8446)	0. 8659 (0.8505 to 0.8812)	0.4436 (0.3914 to 0.5117)	37.31 (33.62 to 41.92)
23°C, 90 min of 3% CO_2: off, two-phase decay	3.081 (2.789 to 3.373)	0.8042 (0.7939 to 0.8146)	0.7281 (0.6759 to 0.7802)	1.175 (0.9174 to 1.6328)	18.85 (15.96 to 23.02)
23°C, 30 min of 3% CO_2: off, two-phase decay	2.706 (2.359 to 3.054)	0.7571 (0.7429 to 0.7713)	0.6327 (0.5052 to 0.7603)	0.6614 (0.3671 to 3.335)	7.884 (6.046 to 11.33)
33°C, 300 min of 3% CO_2: on, two-phase association	−0.07863 (−0.09996 to −0.05729)	0.7646 (0.7517 to 0.7775)	0.3925 (0.3574 to 0.4276)	0.9709 (0.7429 to 1.199)	51.44 (45.07 to 57.82)
33°C, 300 min of 3% CO_2: off, two-phase decay	3.901 (3.651 to 4.151)	0.8595 (0.8536 to 0.8654)	0.8569 (0.8395 to 0.8742)	1.202 (1.066 to 1.376)	32.01 (28.53 to 36.46)
33°C, 90 min of 3% CO_2: off, two-phase decay	3.453 (3.230 to 3.676)	0.8307 (0.8161 to 0.8453)	0.8906 (0.8763 to 0.9049)	1.548 (1.376 to 1.768)	46.43 (37.28 to 61.52)
33°C, 30 min of 3% CO_2: off, two-phase decay	3.025 (2.797 to 3.252)	0.8099 (0.7925 to 0.8273)	0.8756 (0.8425 to 0.9086)	1.537 (1.299 to 1.880)	20.23 (14.45 to 33.71)

τ, time constant; τ_1, fast time constant; τ_2, slow time constant.
Parameter estimates for one- or two-phase exponential equations fitted to RER data using weighted least-squares method with 95% confidence intervals in parentheses.

Fig. 5 shows the ventilatory response to hypoxia. There was no significant effect of 10% O_2 on neither $\dot{V}_E$, f_R nor V_T (P=0.639, P=0.413, P=0.823, respectively, t-test), whereas 5% O_2 had a significant effect on $\dot{V}_E$ and V_T (P=0.015 and P=0.016, respectively, t-test) but not on f_R (P=0.623, t-test). Following re-exposure to normoxia after 5% O_2, $\dot{V}_E$ tended to be reduced due to lower f_R (see Fig. 5).

Effects of duration of hypercapnia and body temperature

Fig. 6 shows results for gas exchange (Fig. 6A–C) and ventilation (Fig. 6D–F) for control, exposure to hypercapnia (3% CO_2) and upon re-exposure to normocapnia at 23 and 33°C. There was a significant effect of hypercapnia and temperature on $\dot{V}_E$ and V_T (P<0.0001 and P=0.0357, P=0.0003 and P=0.0445, respectively, two-way ANOVA), in contrast to f_R (P=0.273 and P=0.884, respectively, two-way

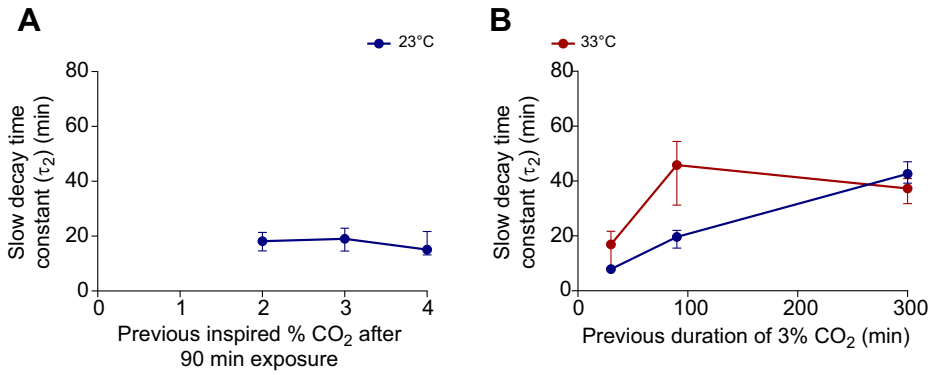

Fig. 2. Fitted slow time constants (τ_2) for decays after hypercapnia. The results for the slow decay time constant (τ_2) fitted with robust method (means with Monte Carlo generated confidence intervals) for all animals combined as a function of the previous level of hypercapnia (i.e. inspired percentage CO_2) (A) and as a function of the previous duration of hypercapnia (B) at 23 and 33°C as indicated. The time constant was unaffected by the previous level of hypercapnia [P=0.314 (ANOVA) when comparing fits for individual animals (not shown)]. However, there was a significant effect of duration of hypercapnia [P=0.0018 in two-way ANOVA for individual fits (not shown) and non-overlapping confidence intervals at 23°C] but no significant effect of temperature [P=0.489 in two-way ANOVA for individual fits (not shown) and overlapping confidence intervals]. N=6.

Journal of Experimental Biology (2016) 219, 3810-3821 doi:10.1242/jeb.143537

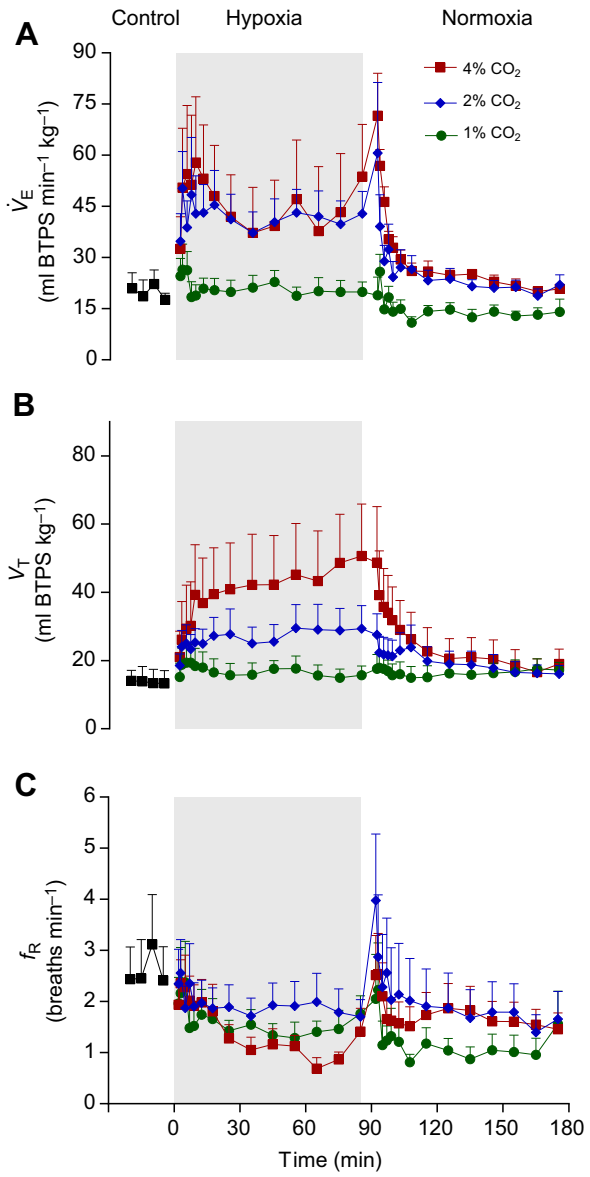

Fig. 3. Ventilatory responses to hypercapnia. Ventilatory responses before, during and after exposure to different levels of hypercapnia at 23°C as indicated, where panel A shows $\dot{V}_E$, panel B shows V_T and panel C is f_R (means±s.e.m.). Whereas V_T was significantly elevated by hypercapnia (P=0.002, one-way repeated measures ANOVA), neither f_R nor $\dot{V}_E$ was significantly different from control (P=0.381 and P=0.156, respectively, one-way repeated measures ANOVA) even though there was a clear tendency for elevated $\dot{V}_E$ at 2 and 4% CO_2. N=6.

ANOVA), but there was no significant interactive effects. RER and $\dot{V}_{CO_2,b}$ were initially reduced, but approached a plateau in a two-phase exponential manner (see 'on' in Table 2C for fitted values for RER). However, a reliable fit could only be made to data at 33°C, whereas the fit was ambiguous at 23°C and hence is not shown in Table 2. Upon re-exposure to normocapnia, RER and $\dot{V}_{CO_2,b}$ immediately increased and approached a plateau, which could be quantified by a two-phase exponential decay (see 'off' in Table 2C). Similarly, upon exposure to shorter durations of hypercapnia (30 and 90 min) RER could be quantified by a two-phase exponential decay (see Table 2C and Fig. 7A,B for decays).

Fig. 2B shows the mean slow time constant with 95% confidence intervals for the decays as a function of the previous duration of hypercapnia (3% CO_2) at 23 and 33°C for the combined fits for all animals (fitted with the robust method). Both weighted least-square fits to the combined data and robust fits to data from individual animals produced very similar result and are therefore not shown. At both 23 and 33°C, the slow time constant for the decays increased with the previous duration of exposure of hypercapnia when comparing the results for individual fits (P=0.0018, two-way ANOVA) (not shown); however, there were no significant effects of temperature (P=0.346, two-way ANOVA) and no significant interactive effects (P=0.489, two-way ANOVA). At 23°C, the significant effect of duration of hypercapnia was also indicated by non-overlapping confidence intervals for the combined robust fits (Fig. 2B); however, at 33°C, the results were less clear because the confidence intervals did overlap. There were no statistically significant effects of the previous duration of hypercapnia or body temperature on mean $\dot{V}_E$ (P=0.958 and P=0.262, respectively, two-way ANOVA). Similarly, for V_T, although there was a tendency for higher V_T at higher temperature, the P-values were just above the level of significance (P=0.645, P=0.051, respectively, two-way ANOVA).

DISCUSSION

Our measurements reveal distinct and prolonged periods in which RER differed markedly from steady state (i.e. ideally RQ) following hypercapnia and hypoxia, indicating pronounced changes in bodily gas stores. The two-compartment model of bodily CO_2 stores (Appendix) predicts the two-phase exponential dynamics of the measured $\dot{V}_{CO_2,b}$ and RER values during and after hypercapnia. The fitted fast and slow time constants for the decay after longer exposure to hypercapnia correspond reasonably well with the model predictions (e.g. Table 2 and Fig. S1) and are similar to values obtained from anaesthetized dogs and humans (Khambatta and Sullivan, 1974; Sullivan et al., 1964, 1966). The time constants for the decay were similar and were not affected by the previous inspired percentage CO_2 concomitant with similar rates of ventilation. The slow time constants were not reduced at higher body temperature as predicted, however, probably as a consequence of lack of temperature effect on ventilation rates during the decays. The increase in the slow time constant with duration of hypercapnia also deviates from the simple model predictions. However, this tends to agree with studies on mammals, where the effective/apparent storage capacities of tissues increase with exposure time due to gradual recruitment of tissues with low perfusion relative to storage capacity (Cherniack et al., 1972; Farhi and Rahn, 1960; Vance and Fowler, 1960). The present results could also suggest that the discrepancy is particularly pronounced at low body temperature as a consequence of the generally slower rates of chemical reactions and perfusion to tissues. Our findings of the extended periods required to reach steady state pertains to the design of experimental protocols to study ventilatory control. The prolonged lack of steady state is particularly relevant to studies involving repetitive exposures with short intervals, such as intermittent hypoxia, where CO_2 stores are unlikely to be restored between individual exposures if these are in the order of minutes to a few hours. The progressive build-up of CO_2 during hypercapnia is also relevant to respirometry, where the rate of CO_2 excretion is likely to be underestimated (Malte et al., 2016b).

Effects of inspired P_{CO_2} on gas exchange and ventilatory response to hypercapnia

Hypercapnia typically elevates V_T in reptiles, whereas attending reductions in f_R may lead to an overall increase or sometimes

Journal of Experimental Biology (2016) 219, 3810-3821 doi:10.1242/jeb.143537

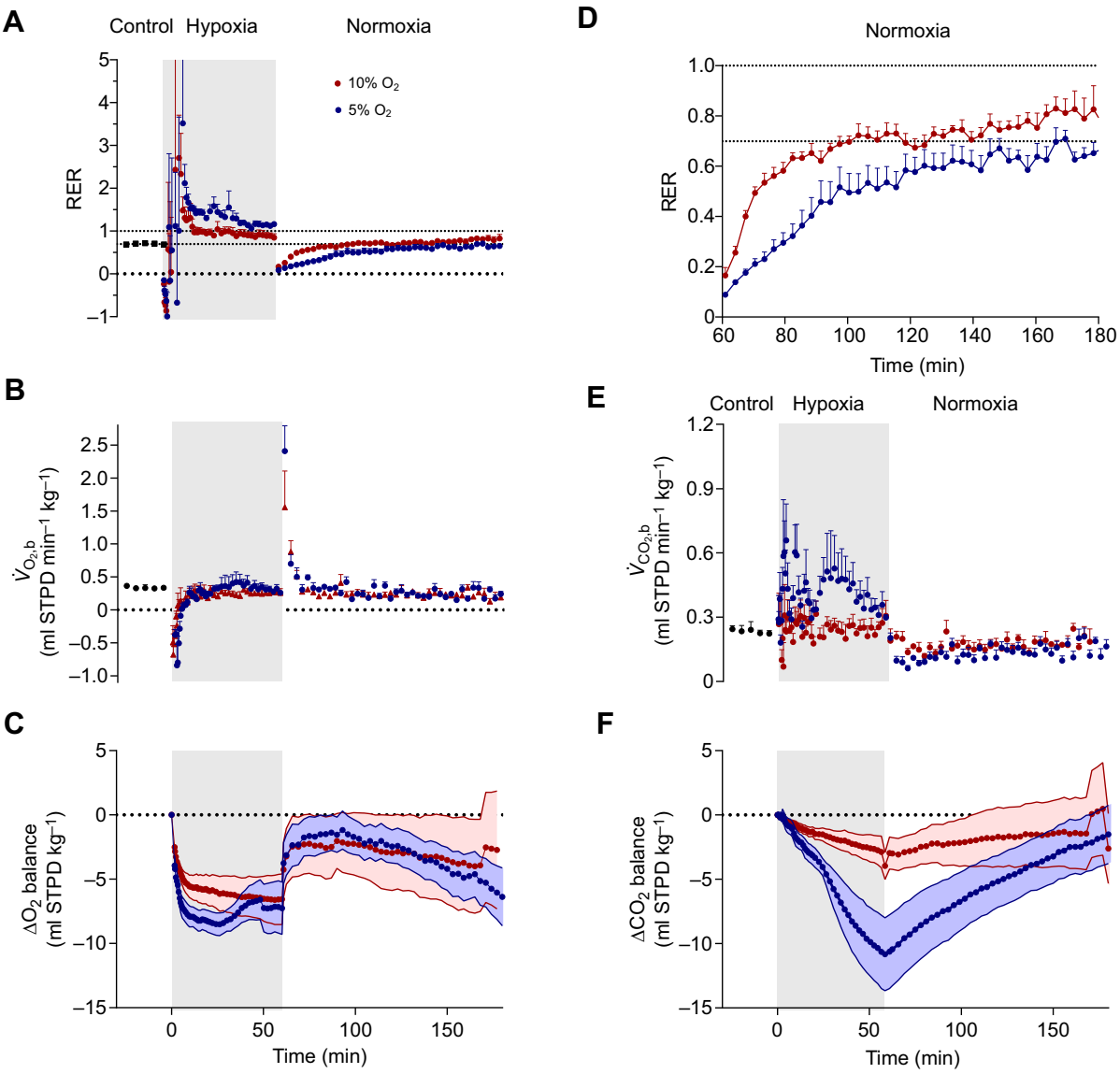

Fig. 4. Gas exchange responses to hypoxia. Gas exchange (means±s.e.m.) before, during and after exposure to different levels of hypoxia at 23°C. (A–C) RER, $\dot{V}_{O_2,b}$ and the estimated change in O_2 balance are shown, respectively. (D) Zoomed-in version of panel A for the changes in RER upon returning to normoxia after hypoxia. (E,F) $\dot{V}_{CO_2,b}$ and the estimated change in CO_2 balance are shown. At the end of exposure to 10% O_2, $\dot{V}_{O_2,b}$, $\dot{V}_{CO_2,b}$ and RER were not significantly different from control (P=0.079, P=0.363, P=0.140, respectively, paired t-test), in contrast to exposure to 5% O_2, where $\dot{V}_{O_2}$, $\dot{V}_{CO_2}$ and RER were all elevated (P=0.029, P=0.0003, P=0.002, respectively, paired t-tests). Upon re-exposure to normoxia, the estimated time to reach 63% of the pre-hypoxic control RER after 5% O_2 (40.4±10.2 min) was significantly longer than after 10% O_2 (9.0±2.0 min) (P=0.031, Wilcoxon matched pairs). For the exposure to 10% O_2, N=5; otherwise, N=6.

even a decrease in $\dot{V}_E$ (de Andrade et al., 2004; Milsom et al., 2004; Nielsen, 1961; Tattersall et al., 2006; Wang and Warburton, 1995). We also observed rather variable ventilatory responses among individuals at 4% CO_2, and the small ventilatory response may have contributed to a slow course of gas exchange, so steady state was not reached within 90 min at 4% CO_2 as indicated by RER remaining considerable lower than the possible RQ range.

The observation that the slow time constant (Fig. 2A) was unaffected by the level of hypercapnia indicates a similar relative speed of readjusting the CO_2 stores despite the differences in CO_2 retention. This is expected for constant storage capacities and similar rates of ventilation and blood flow. Even though the mean $\dot{V}_E$ and V_T for the decays did not differ between 2, 3 and 4% CO_2, V_T tended to be transiently elevated after 4% as compared to 2% CO_2, leading to presumably higher effective ventilation, which could have reduced the time constants. Furthermore, RER remained high (>0.9) even 1.5 h after the return to normocapnia for some animals after 4% CO_2, probably indicating that the CO_2 stores were still not fully readjusted. If so, this may have influenced our data and may have affected the non-linear regression and thus pose a larger uncertainty on the estimated time constants after 4% CO_2. Furthermore, immediately after changes in CO_2 levels, $\dot{V}_{O_2,b}$ tended to show fast transient changes that probably affect the fit to RER, leading to deviations from those expected on the CO_2 dynamics alone.

Effects of body temperature and duration of hypercapnia on gas exchange

Given that 'alveolar' ventilation and blood flow increase with body temperature in ectotherms in combination with a slight reduction in

Journal of Experimental Biology (2016) 219, 3810-3821 doi:10.1242/jeb.143537

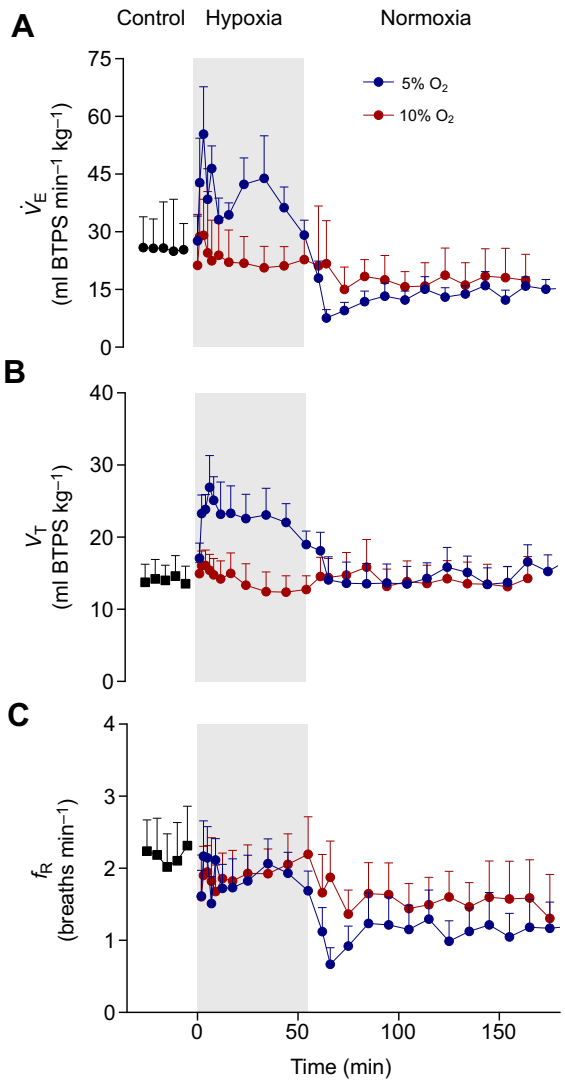

Fig. 5. Ventilatory responses to hypoxia. Ventilatory responses (means± s.e.m.) before, during and after exposure to different levels of hypoxia at 23°C as indicated, where panel A shows $\dot{V}_E$, panel B shows V_T and panel C is f_R. At 10% O_2, neither $\dot{V}_E$, V_T nor f_R were significantly different from control (P=0.637, P=0.823, P=0.413, paired t-tests). At 5% O_2, both $\dot{V}_E$ and V_T were significantly elevated (P=0.0015, P=0.016, paired t-tests) compared to control, in contrast to f_R (P=0.623, paired t-test). N=6.

CO_2 capacitance coefficients of the body fluids (Dejours, 1981; Jackson, 1971; Smith, 1975), it would be expected that time constants were reduced (Fig. S1C,D). However, we did not find significant effects of temperature on the time constants, which is likely to be a consequence of the lack of temperature effect on $\dot{V}_E$ in the transients. A further explanation for the similar slow time constants could be that elevated perfusion and the higher rates of chemical reactions at 33°C recruited tissue effective storage capacity relative to that at 23°C (as elaborated in the next paragraph). Indeed, a complete steady state might not have been attained even 300 min into the exposure to hypercapnia at 23°C, and the two-phase exponential fit was ambiguous. However, gas exchange data for the exposure to hypercapnia may be more uncertain and have larger variation, given the higher rates of $\dot{V}_E$ relative to metabolism (especially at lower body temperature) that may reduce the signal-to-noise ratio for analyzing breath-to-breath gas exchange.

The increase in the slow decay time constant with duration of hypercapnia, despite similar mean $\dot{V}_E$ and V_T (and hence alveolar ventilation and presumable blood flow), is in contrast to the model predictions. Consequently, this could indicate that tissue CO_2 storage is not homogeneous/uniform with a fixed effective storage capacity but instead that storage takes place in multiple distinct compartments with different ratios of perfusion (and diffusion) conductance relative to storage capacity (Farhi and Rahn, 1960). This interpretation would tend to agree with studies on mammals, in which the effective/apparent storage capacity may gradually increase with exposure time due to temporal recruitment of tissues with low perfusion relative to storage capacity that may be effectively unavailable for storage at short exposures (Cherniack et al., 1972; Farhi and Rahn, 1960; Vance and Fowler, 1960). The discrepancy between the slow time constants and duration of hypercapnia was less pronounced at 33°C, in agreement with presumably higher rates of perfusion and faster rates of chemical reactions that could lead to more homogenous CO_2 storage. Although the fitted slow time constants for the decays tended to reach a plateau or final value as a function of the duration of hypercapnia at 33°C, this might not have been the case at 23°C. Consequently, it is possible that longer exposures (beyond 300 min) would increase the time constant further.

It could be expected that the predicted slow time constants (see Model predictions paragraph above and Fig. 1A,D) would underestimate the fitted values (see Table 2) since the model assumes an ideal system without diffusion limitations, ventilation perfusion heterogeneity and shunts. Given that this was not the case, it could further indicate that the apparent/effective bodily storage capacity is less than expected. However, derivation of the analytic solution also assumes a constant unregulated system, i.e. with constant resistances and hence rates of ventilation, which is in contrast to a ventilatory off-response following hypercapnia that could reduce the effective time constant for attainment of steady state. More elaborate numerical models that incorporate multiple tissue compartments, limitations imposed by diffusion, regulation of ventilation etc. (e.g. Cherniack and Longobardo, 1970; Farhi and Rahn, 1960; Malte et al., 2016a,b; Stephenson, 2005) would improve predictive power at the expense of simple analytic solutions.

Effects of hypoxia on gas exchange and ventilation

In agreement with previous studies, 10% O_2 did not stimulate ventilation and a new steady state of gas exchange was apparently established (Skovgaard and Wang, 2004, 2007; Wang and Warburton, 1995). However, at the end of the exposure to 5% O_2, RER remained above 1 and was significantly different from control due to an elevated $\dot{V}_{CO_2,b}$ caused by the hyperventilation. The slower time course for RER during re-exposure to normoxia after 5% O_2 was probably due to the transient reduction in ventilation following re-exposure to normoxia. Thus, concomitantly with the reloading of O_2 stores, the reduction in ventilation appeared to lead to a compensatory hypoventilation that reloaded the CO_2 stores that were previously eliminated due to hyperventilation during 5% O_2. The slow time course for CO_2 adjustments for a hypoventilation is also expected from the model (Appendix and Fig. 1C,D), predicting a hyperbolic-like relation between time constant and ventilation so that even small reductions in ventilation compared to the normal ventilation rate may lead to significantly longer time constants.

Implications for experimental design

Upon shorter exposures (<90 min) to 2% CO_2 and above, a steady state for gas exchange and thus the CO_2 stores of the body cannot

Journal of Experimental Biology (2016) 219, 3810-3821 doi:10.1242/jeb.143537

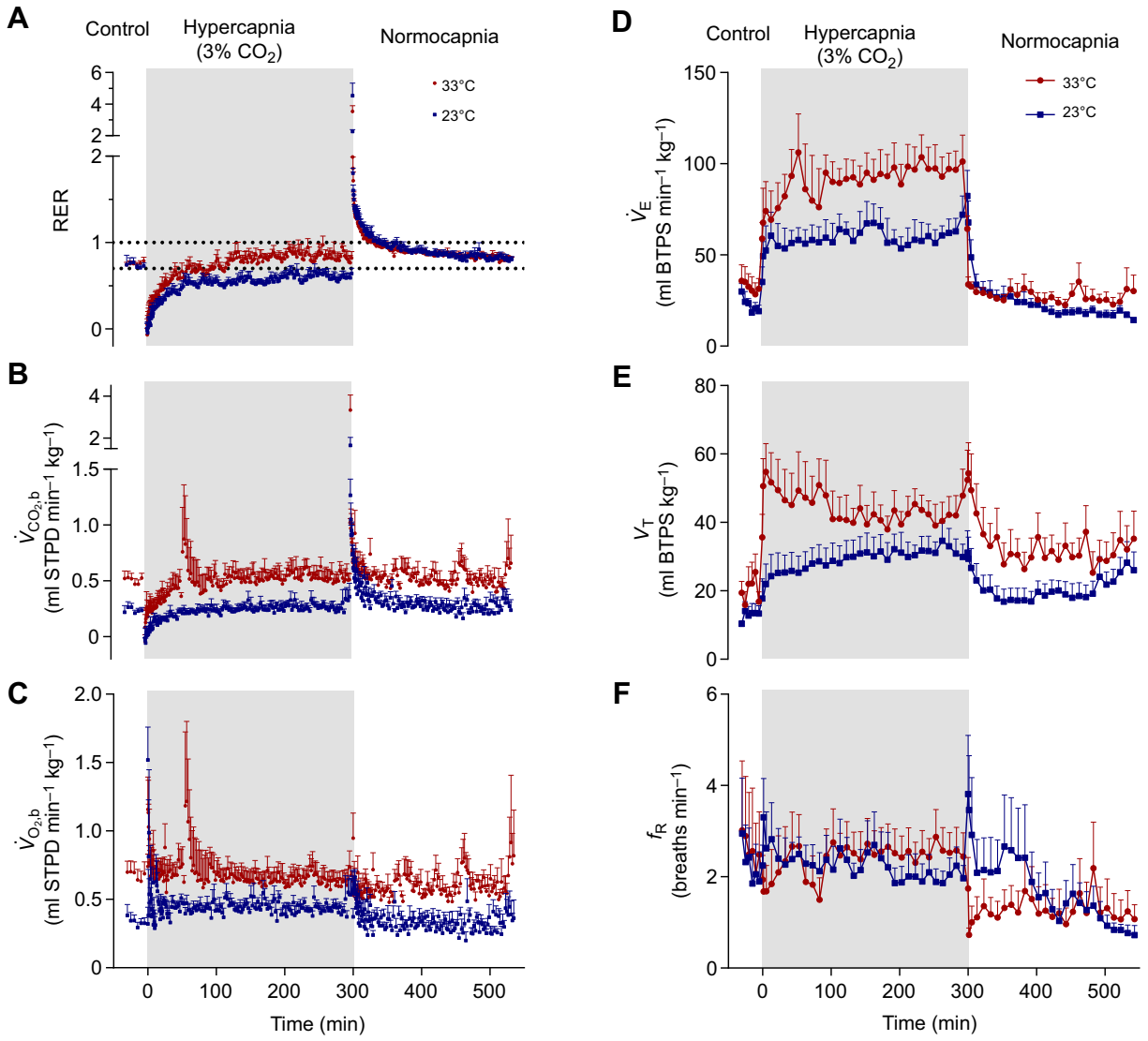

Fig. 6. Gas exchange and ventilatory responses to 3% CO_2 at 23°C and 33°C. (A–C) RER, $\dot{V}_{CO_2,b}$ and $\dot{V}_{O_2,b}$ (means+s.e.m.) are shown, respectively. The dotted lines in A indicate the physiological RQ range (0.7–1). (D–F) $\dot{V}_E$, V_T and f_R before, during and after 300 min exposure to 3% CO_2 at 23°C and 33°C are shown. There was a significant effect of hypercapnia and temperature on $\dot{V}_E$ (P<0.0001, P=0.0357, respectively, two-way ANOVA) and V_T (P=0.0003, P=0.0445, respectively, two-way ANOVA). For the responses during exposure to hypercapnia, N=5; otherwise, N=6.

necessarily be expected, particularly if the rates of blood flow and ventilation are low (typical of low body temperature). Consequently, P_{CO_2} in the bodily compartments (tissues, blood and lungs) may not have reached their final steady state values and, thus, the full stimulatory effect of elevated arterial P_{CO_2} (Pa_{CO_2}) on ventilation may not be exerted. Similarly, if not allowing sufficient time for readjustment of the gas stores upon re-exposure to normocapnia and normoxia after hypercapnia or hypoxia, there may still be a residual drive/inhibition on ventilation. This is particularly important when interpreting ventilatory responses during repeated intermittent

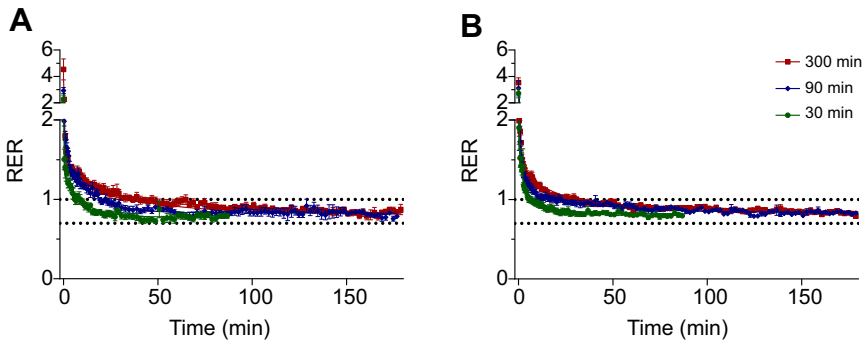

Fig. 7. RER for decays following varying durations of exposure to 3% CO_2 at 23°C and 33°C. RER (means± s.e.m.) upon the return to normocapnia after exposure to varying durations of hypercapnia at 23°C (A) and 33°C (B) with fitted two-phase exponential functions. The dotted lines indicate the physiological RQ range (0.7–1). See Table 2 for fitted parameters made to combined data from all animals with weighted least-squares method and Fig. 2B for fitted slow time constants with robust method and Monte Carlo-acquired confidence intervals. N=6.

exposures to hypoxia or hypercapnia, where a gradual accumulation or depletion of CO_2 stores may develop unless sufficient time is allowed for in between exposures. The slow transient adjustment of CO_2 stores leading to RER values different from steady state may also lead to erroneous interpretations regarding tissue CO_2 production and hence RQ of the tissues if assuming a steady state (Malte et al., 2016b). The tendency for this may be greatest during hypoventilation, where time constants are long due to the low ventilation rates (Fig. S1C,D). Furthermore, longer exposure to inspired hypercapnia and higher inspired P_{CO_2} may require a relatively longer time for eliminating the error on $\dot{V}_{CO_2,b}$ and RER due to potentially larger total error/disturbance (larger bodily CO_2 accumulation) and longer or similar time constants. However, a high ventilatory off-response (dependent on Pa_{CO_2}) during the decay after hypercapnia would theoretically be predicted to reduce the time constants and hence promote a faster attainment of steady state.

Conclusions

Our experimental results demonstrate pronounced transient gas exchange during and after hypoxia and hypercapnia. For hypercapnia, the transients were adequately described by two-phase exponential functions for RER. A simple two-compartment model predicts the two-phase exponential dynamics, and the predicted values of the time constants concur reasonably well with the fitted values from experimental data after prolonged hypercapnia. The slow time constants for the decays were not affected by the level of hypercapnia and they were not shortened at higher body temperatures (33 versus 23°C), which probably reflected lack of temperature effect on ventilation rates for the decays. Furthermore, the slow time constants for the decays increased with the previous duration of hypercapnia, which was mostly pronounced at low body temperature. This contrasts with the model predictions and could indicate a temporal recruitment of the apparent/effective storage capacity, as in mammals (Cherniack et al., 1972; Farhi and Rahn, 1960; Vance and Fowler, 1960). We conclude that attainment of a steady state requires considerable time in reptiles, and this has important implications for designing experimental protocols when conducting respirometry and studying ventilatory control.

APPENDIX

Two-compartment model of changes in bodily CO_2 stores

If venous blood and tissues (subscript v) as well as arterial blood and the lung (subscript a) are joined as two combined compartments, respectively (similar to Farhi and Rahn, 1960 and Longobardo et al., 1967), the following differential equations can be derived from mass balances:

$$\frac{dPv_{CO_2}(t)}{dt} = \frac{\dot{V}_{CO_2}}{C_v} - \frac{Pv_{CO_2}(t) - Pa_{CO_2}(t)}{C_v R_{perf}}, \quad (A1)$$

$$\frac{dPa_{CO_2}(t)}{dt} = \frac{Pv_{CO_2}(t) - Pa_{CO_2}(t)}{C_a R_{perf}} - \frac{Pa_{CO_2}(t) - PI_{CO_2}}{C_a R_{vent}}. \quad (A2)$$

Joining the compartments rests on the assumption of complete equilibration between all venous blood and tissues and all arterial blood and lung air (which is strictly not true during non-steady state), as well as constant blood and tissues capacitance coefficients, which is approximately true for CO_2. In Eqns A1 and A2, P is partial pressure, C is storage capacity (product of specific capacitance, β, and compartmental size, V), R_{vent} and R_{perf} are the ventilatory and perfusive resistance, and $\dot{V}_{CO_2}$ is the CO_2 production rate. The storage capacities and resistances are given in Table 1 along with other abbreviations.

The non-homogenous linear system of differential Eqns A1 and A2 can be solved by conventional methods. By differentiating Eqn A2 and combining with Eqn A1, a single non-homogenous second-order equation is obtained:

$$\frac{d^2Pa_{CO_2}(t)}{dt^2} + \frac{dPa_{CO_2}(t)}{dt} \times (b + c + d) + Pa_{CO_2}(t) \times b \times d = PI_{CO_2} b \times d + a \times c, \quad (A3)$$

where a, b, c and d are lumped parameters of Eqn A1 and A2 (see Table 1). For constant parameters, the solution to Eqn A3 is given below (for example, see O'neil, 2011):

$$Pa_{CO_2}(t) = PI_{CO_2} + \dot{V}_{CO_2} R_{vent} + K_1 \exp\left(-\frac{t}{\tau_1}\right) + K_2 \exp\left(-\frac{t}{\tau_2}\right), \quad (A4)$$

where K_1 and K_2 are determined from initial conditions and the lumped parameters (see Table 1), and τ_1 and τ_2 are the fast and slow time constant, respectively (see Table 1). The rate of CO_2 excretion [$\dot{V}_{CO_2,b}(t)$] is then given by:

$$\dot{V}_{CO_2,b}(t) = \frac{[Pa_{CO_2}(t) - PI_{CO_2}]}{R_{vent}}$$

$$\Updownarrow \quad (A5)$$

$$\dot{V}_{CO_2,b}(t) = \dot{V}_{CO_2} + A_1 \exp\left(-\frac{t}{\tau_1}\right) + A_2 \exp\left(-\frac{t}{\tau_2}\right),$$

where A_1 and A_2 are the spans in $\dot{V}_{CO_2,b}$ for τ_1 and τ_2, respectively (see Table 1; Fig. S1).

Competing interests

The authors declare no competing or financial interests.

Author contributions

C.L.M. conducted the experimental measurements but otherwise all authors contributed equally.

Funding

This research was supported by the Danish Natural Science Research Council (FNU; Natur og Univers, Det Frie Forskningsråd).

Supplementary information

Supplementary information available online at http://jeb.biologists.org/lookup/doi/10.1242/jeb.143537.supplemental

References

Boutilier, R. (ed.) (1990). Control and co-ordination of gas exchange in bimodal breathers. In *Vertebrate Gas Exchange*, pp. 279-345. Berlin: Springer.

Boutilier, R., Reed, J. and Fedak, M. (2001). Unsteady-state gas exchange and storage in diving marine mammals: the harbor porpoise and gray seal. *Am. J. Physiol. Regul. Integr. Comp. Physiol.* **281**, R490-R494.

Burggren, W. W. and Shelton, G. (1979). Gas exchange and transport during intermittent breathing in chelonian reptiles. *J. Exp. Biol.* **82**, 75-92.

Cherniack, N. S. and Longobardo, G. (1970). Oxygen and carbon dioxide gas stores of the body. *Physiol. Rev.* **50**, 196-243.

Cherniack, N. S., Tuteur, P. G., Edelman, N. H. and Fishman, A. P. (1972). Serial changes in CO_2 storage in tissues. *Respir. Physiol.* **16**, 127-141.

de Andrade, D. V., Tattersall, G. J., Brito, S. P., Soncini, R., Branco, L. G., Glass, M. L., Abe, A. S. and Milsom, W. K. (2004). The ventilatory response to environmental hypercarbia in the South American rattlesnake, Crotalus durissus. *J. Comp. Physiol. B* **174**, 281-291.

Dejours, P. (1981). *Principles of Comparative Respiratory Physiology: Sole Distributors for the USA and Canada*. Amsterdam: Elsevier.
Farhi, L. and Rahn, H. (1955). Gas stores of the body and the unsteady state. *J. Appl. Physiol.* **7**, 472-484.
Farhi, L. E. and Rahn, H. (1960). Dynamics of changes in carbon dioxide stores. *Anesthesiology* **21**, 604-614.
Garland, R. J. and Milsom, W. K. (1994). End-tidal gas composition is not correlated with episodic breathing in hibernating ground squirrels. *Can. J. Zool.* **72**, 1141-1148.
Glass, M. L. and Johansen, K. (1979). Periodic breathing in the crocodile, *Crocodylus niloticus*: consequences for the gas exchange ratio and control of breathing. *J. Exp. Zool.* **208**, 319-325.
Glass, M. L. and Wood, S. C. (1983). Gas exchange and control of breathing in reptiles. *Physiol. Rev* **63**, 425-427.
Glass, M. L., Wood, S. C. and Johansen, K. (1978). The application of pneumotachography on small unrestrained animals. *Comp. Biochem. Physiol. A Physiol.* **59**, 425-427.
Hicks, J. W. and Wang, T. (1999). Hypoxic hypometabolism in the anesthetized turtle, Trachemys scripta. *Am. J. Physiol. Regul. Integr. Comp. Physiol.* **277**, R18-R23.
Jackson, D. C. (1971). The effect of temperature on ventilation in the turtle, Pseudemys scripta elegans. *Respir. Physiol.* **12**, 131-140.
Khambatta, H. J. and Sullivan, S. F. (1974). Carbon dioxide production and washout during passive hyperventilation alkalosis. *J. Appl. Physiol.* **37**, 665-669.
Longobardo, G. S., Cherniack, N. S. and Staw, I. (1967). Transients in carbon dioxide stores. *Biomed. Eng. IEEE Trans.* **14**, 182-191.
Malte, C. L., Jakobsen, S. L. and Wang, T. (2014). A critical evaluation of automated blood gas measurements in comparative respiratory physiology. *J. Comp. Physiol. A* **178**, 7-17.
Malte, C. L., Malte, H. and Wang, T. (2016a). Periodic ventilation: consequences for the bodily CO_2 stores and gas exchange efficiency. *Respir. Physiol. Neurobiol.* **231**, 63-74.
Malte, C. L., Nørgaard, S. and Wang, T. (2016b). Closed system respirometry may underestimate tissue gas exchange and bias the respiratory exchange ratio (RER). *J. Comp. Physiol. A* **192**, 17-27.
Milsom, W. K. (1991). Intermittent breathing in vertebrates. *Annu. Rev. Physiol.* **53**, 87-105.
Milsom, W. K., Abe, A. S., Andradeb, D. V. and Tattersall, G. J. (2004). Evolutionary trends in airway CO_2/H^+ chemoreception. *Respir. Physiol. Neurobiol.* **144**, 191-202.
Motulsky, H. J. and Brown, R. E. (2006). Detecting outliers when fitting data with nonlinear regression–a new method based on robust nonlinear regression and the false discovery rate. *BMC Bioinform.* **7**, 123.
Motulsky, H. and Christopoulos, A. (2004). *Fitting Models to Biological Data Using Linear and Nonlinear Regression: A Practical Guide to Curve Fitting*. Oxford: Oxford University Press.
Nielsen, B. (1961). On the regulation of the respiration in reptiles the effect of temparature and Co2 on the respiration of lizards (Lacerta). *J. Exp. Biol.* **38**, 301-314.
O'neil, P. V. (2011). *Advanced Engineering Mathematics*. Stamford: Cengage learning.
Porteus, C., Hedrick, M. S., Hicks, J. W., Wang, T. and Milsom, W. K. (2011). Time domains of the hypoxic ventilatory response in ectothermic vertebrates. *J. Comp. Physiol. B* **181**, 311-333.
Shelton, G. and Boutilier, R. (1982). Apnoea in amphibians and reptiles. *J. Exp. Biol.* **100**, 245-273.
Shelton, G. and Croghan, P. C. (1988). Gas exchange and its control in non-steady-state systems: the consequences of evolution from water to air breathing in the vertebrates. *Can. J. Zool.* **66**, 109-123.
Shelton, G., Jones, D. R. and Milsom, W. K. (1986). Control of breathing in ectothermic vertebrates. In: *Handbook of Physiology* (ed. A. P. Fishman), pp. 857-909. Baltimore: William & Wilkins Company.
Skovgaard, N. and Wang, T. (2004). Cost of ventilation and effect of digestive state on the ventilatory response of the tegu lizard. *Respir. Physiol. Neurobiol.* **141**, 85-97.
Skovgaard, N. and Wang, T. (2007). Low cost of ventilation in the vagotomised alligator (Alligator mississippiensis). *Respir. Physiol. Neurobiol.* **159**, 28-33.
Smith, E. N. (1975). Oxygen consumption, ventilation, and oxygen pulse of the American alligator during heating and cooling. *Physiol. Zool.* **48**, 326-337.
Stephenson, R. (2005). Physiological control of diving behaviour in the Weddell seal *Leptonychotes weddelli*: a model based on cardiorespiratory control theory. *J. Exp. Biol.* **208**, 1971-1991.
Stinner, J. N. and Wardle, R. L. (1988). Effect of temperature upon carbon dioxide stores in the snake Coluber constrictor and the turtle Chrysemys scripta. *J. Exp. Biol.* **137**, 529-548.
Stinner, J., Hartzler, L. K., Grguric, M. and Newlon, D. (1998). A protein titration hypothesis for the temperature-dependence of tissue CO2 content in reptiles and amphibians. *J. Exp. Biol.* **201**, 415-424.
Sullivan, S., Patterson, R. and Papper, E. (1964). Tissue carbon dioxide stores: magnitude of acute change in the dog. *Am. J. Physiol.* **206**, 887-890.
Sullivan, S., Patterson, R. and Papper, E. (1966). Arterial CO2 tension adjustment rates following hyperventilation. *J. Appl. Physiol.* **21**, 247-250.
Tattersall, G. J., de Andrade, D. V., Brito, S. P., Abe, A. S. and Milsom, W. K. (2006). Regulation of ventilation in the caiman (Caiman latirostris): effects of inspired CO_2 on pulmonary and upper airway chemoreceptors. *J. Comp. Physiol. B* **176**, 125-138.
Vance, J. W. and Fowler, W. S. (1960). Adjustment of stores of carbon dioxide during voluntary hyperventilation. *Dis. Chest* **37**, 304-313.
Wang, T. and Warburton, S. J. (1995). Breathing pattern and cost of ventilation in the American alligator. *Respir. Physiol.* **102**, 29-37.
Wang, T., Smits, A. and Burggren, W. W. (1998). Pulmonary function in reptiles. *Biol. Reptilia* **19**, 297-374.
Weinstein, Y., Ackerman, R. A. and White, F. N. (1986). Influence of temperature on the CO_2 dissociation curve of the turtle *Pseudemys scripta*. *Respir. Physiol.* **63**, 53-63.

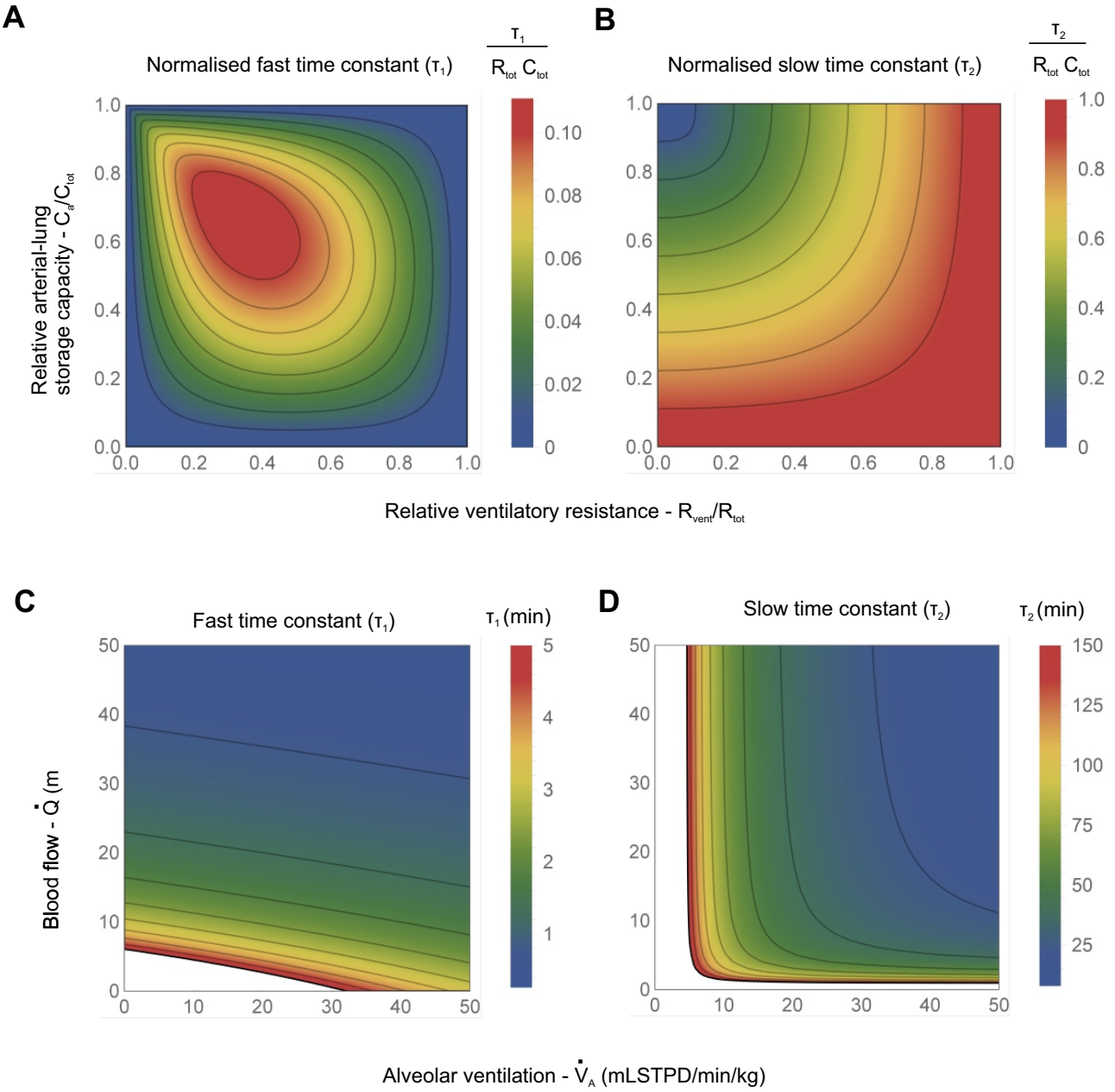

Fig. S1. Modelling results for fast (τ_1) and slow (τ_2) time constants. Modelling results showing density plots illustrating the effects of storage capacities and resistances on the fast (τ_1) and slow (τ_2) time constants. Panels A and B show the fast time and slow time constant, respectively, divided to the product of the total resistance (R_{tot}=R_{perf}+R_{vent}) and total storage capacity (C_{tot}=C_a+C_v) as a function of the relative ventilatory resistance (i.e. R_{vent}/R_{tot}, horizontal axis) and the relative arterial-lung storage capacity (i.e. C_a/C_{tot}), vertical axis). Panels B and C show the effects of alveolar ventilation (horizontal axis) and blood flow (vertical axis) on the fast and slow time constant, respectively. Panels A and B illustrate that the presence of a fast and slow time constant is the result of the distribution of the total storage capacity at two distinct compartments with a finite blood convective resistance in between. When blood flow and alveolar ventilation increase, both the fast and slow time constant is reduced and vice versa (panels C and D). Input parameters used for panels C and D: Arterial blood volume (V_a)=15 ml, Venous blood volume (V_v)=45 ml, Lung volume (V_A)=100 mlSTPD, available tissues storage capacity (V_{Tis} β_T)=0.46 mlSTPD/mmHg (similar to estimates from turtles (Burggren and Shelton, 1979), see also (Cherniack and Longobardo, 1970; Farhi and Rahn, 1955)), air CO_2 capacitance coefficient (β_g)=1/739 ml CO_2/ml air/mmHg, Blood CO_2 capacitance coefficient (β_b)=0.0055 mlSTPD $mlblood^{-1}$ $mmHg^{-1}$ (similar to Weinstein et al., 1986).